

# GRAPHICAL ANALYSIS OF NONIDEAL MONOMER *N*-MER, ISODESMIC, AND TYPE II INDEFINITE SELF-ASSOCIATING SYSTEMS BY EQUILIBRIUM ULTRACENTRIFUGATION

WALTER F. STAFFORD, III, *Rosenstiel Basic Medical Sciences Research Center,  
Brandeis University, Waltham, Massachusetts 02154 U.S.A.*

**ABSTRACT** A graphical procedure is described by which one can obtain in principle the monomer molecular weight, stoichiometry, equilibrium constant, and second virial coefficient of nonideal monomer *N*-mer, isodesmic, and type II indefinite self-associating systems. In addition, a method is presented for obtaining both the equilibrium constant and the second virial coefficient from the maximum in a plot of apparent molecular weight vs. concentration if the monomer molecular weight and stoichiometry are known. The usefulness and limitations of the methods are discussed, as well as the quality and range of data required for determination of the relevant parameters. The techniques described are applicable to analysis of self-associating systems by osmotic pressure and light scattering, as well as equilibrium ultracentrifugation measurements.

Earliest theoretical (1) and experimental (2) analyses of self-associating systems in the ultracentrifuge were restricted to ideal systems. Somewhat later attempts to deal with nonideality in these types of systems (3) involved correcting data to their ideal values by using calculated estimates of the second virial coefficient. The first full treatment of a nonideal monomer-dimer system was given by Adams and Fujita (4), who presented an equation for simultaneous determination of both the second virial coefficient and association constant. The first treatment of a nonideal isodesmic indefinite self-association was given by Van Holde and Rossetti (5), who used an iterative method to obtain the second virial coefficient for the self-association of purine. Since then, these workers and others have elaborated their techniques and developed others to deal with more complicated systems. The reader is referred to the reviews and monographs by Adams (6), Yphantis (7), Williams (8), Teller (9), Van Holde (10), Fujita (11), Lewis and Weiss (12), Eisenberg (13), and Kim et al. (14).

There are two general approaches to the analysis of ultracentrifugation data. One involves determination of the moments of mass of the equilibrium distribution and the other involves direct analysis of the mass distribution, either by curve fitting to sums of exponentials over relatively large spans of data (15, 16, 9) or by various graphical techniques (17, 18).

The first method has the advantage that no specific model need be postulated to determine the moments of the mass distribution. The calculated moments then can be used to test for various reaction schemes. The direct fit methods are free from certain possible systematic

---

Dr. Stafford's present address is Department of Muscle Research, Boston Biomedical Research Institute, 20 Staniford Street, Boston, Massachusetts 02114.

errors inherent in the determination of some of the moments, but require that a model be specified. However, once a model has been determined, a direct fit can be used to get relatively precise estimates and error statistics for the parameters of the model. This communication is concerned with a graphical procedure using the moments of the equilibrium mass distribution.

Several graphical methods for analysis of ideal and nonideal self-associating systems employing moments of the equilibrium mass distribution have been reported (19–23). Some of these methods are based on the concept of standard graphs expressed in terms of reduced variables that allow direct comparison with experimental data. The graphical procedure presented in this communication is based on similar concepts, and employs simultaneous graphical fits to several molecular weight moments to yield, in principle, the monomer molecular weight, stoichiometry, equilibrium constant, and second virial coefficient for nonideal monomer  $N$ -mer, isodesmic, and type II indefinite self-associating systems.

### INTRODUCTORY THEORY

In general, it can be shown for a species  $i$  at equilibrium in a centrifugal field in an incompressible solution (24) that

$$M_i(1 - \bar{v}_i\rho)\omega^2 d\xi = d\mu_i, \quad (1)$$

where  $M_i$  is the molecular weight,  $\bar{v}_i$  is the partial specific volume,  $\rho$  is the solution density,  $\omega$  is the angular velocity of the rotor,  $R$  is the gas constant,  $T$  is the absolute temperature,  $\mu_i$  is the chemical potential per mole of species  $i$ , and  $\xi = r^2/2$ .<sup>1</sup> For convenience, (see Yphantis [25]) we define

$$\sigma_i \equiv M_i(1 - \bar{v}_i\rho)\omega^2/RT. \quad (2)$$

The chemical potential of species  $i$  is given by

$$\mu_i = \mu_i^\circ + RT \ln c_i y_i, \quad (3)$$

where  $c_i$  is the concentration of species  $i$  in units of  $\text{g} \cdot \text{cm}^{-3}$ ,  $\mu_i^\circ$  is its standard chemical potential, and  $y_i$  is its activity coefficient that expresses deviations from thermodynamic ideality as well as the effects of the Donnan equilibrium. Deviations from ideality arising through intermolecular association are excluded specifically from  $y_i$  (26). For most purposes, nonideality and Donnan effects can be treated by expanding  $\ln y_i$  in a power series of the total macromolecular concentration and truncating after the linear term (4) such that

$$\ln y_i = 2B\sigma_i c, \quad (4)$$

where  $B$  is the colligative second virial coefficient.

The validity of Eq. 4 for the description of nonideality in self-associating systems depends on the assumption that the contribution to the second virial coefficient of each species is

<sup>1</sup>It is assumed in this treatment that the density increment,  $(1 - \bar{v}_i\rho)$ , is independent of macromolecular concentration. This approximation is valid for most cases encountered in practice (13).

proportional to its mass. This assumption can be made probably quite generally for systems composed of a monomer and its oligomers for those cases in which contributions to the second virial coefficient arise from the Donnan equilibrium, since the charge-to-mass ratio is likely to remain nearly constant on polymerization (27). However, the same assumption, in general, cannot be made for systems in which the excluded volume makes an appreciable contribution. The excluded volume contribution to  $B$  is given by a relation of the form  $B_i = a_i \bar{v}_i / M_i$ , where  $a_i$  is a parameter reflecting the geometry of the molecule. For example (28),  $a_i = 4$  for spheres, and  $a_i = L/d$  (where  $L$  = length and  $d$  = diameter) for rod-shaped molecules. Thus,  $B_i M_i = a_i \bar{v}_i / N_i$ , where  $N_i$  is the stoichiometric coefficient. Therefore, in order that  $B_i M_i$  be a constant,  $a_i$  must be proportional to  $N_i$ . This would be true only for special geometries, such as end-to-end polymerization of rods, and is a constraint that generally is not satisfied. The problem of concentration dependence of  $B$  has been reviewed recently by Eisenberg (13).

To proceed with the theoretical development, we substitute Eqs. 2–4 into Eq. 1 and perform the indicated differentiation, obtaining the following relationship, which will be used to derive the various familiar apparent molecular weight averages:

$$\sigma_i c_i = \frac{dc_i}{d\xi} \frac{1}{\left(1 - 2B \frac{dc}{d\xi}\right)} \quad (5)$$

The series of ideal molecular weight averages,  $\sigma_n$ ,  $\sigma_w$ ,  $\sigma_z$ , and  $\sigma_{z+1}$ , can be calculated from the following definition (29), assuming  $\bar{v}$  and  $dn/dc$  (where  $n$  is the refractive index) are the same for all species:

$$\sigma_{k,id} = \frac{\sum c_i \sigma_i^{j+1}}{\sum c_i \sigma_i^j} \quad (6)$$

where  $j = -1, 0, 1$  and  $2$ , and  $k = n, w, z$ , and  $z + 1$ , respectively. The corresponding apparent molecular weight averages are given by (25)

$$\sigma_{k,app} = \frac{d^{j+1}c/d\xi^{j+1}}{d^j c/d\xi^j}, \quad (7)$$

where  $j$  and  $k$  have the same meaning as above with the proviso that  $j = 0$  refers to no differentiation and  $j = -1$  refers to integration with respect to  $\xi$ .

For the discussion of nonideality and Donnan effects it is useful to define a recurrence relation for deriving relations between the  $\sigma_{k,id}$  and the  $\sigma_{k,app}$ . It can be shown that

$$\sum c_i \sigma_i^{j+1} = \frac{1}{\left(1 - 2B \frac{dc}{d\xi}\right)} \frac{d}{d\xi} \sum c_i \sigma_i^j \quad (8)$$

for  $j = -1, 0, 1$ , and  $2$ . Eq. 8 can be used with Eqs. 6 and 7 to generate the following familiar (9) relationships:

$$\frac{1}{M_{n,app}} = \frac{1}{M_{n,id}} + Bc \quad (9a)$$

$$\frac{1}{M_{w,app}} = \frac{1}{M_{w,id}} + 2Bc \quad (9b)$$

$$\frac{1}{M_{z,app}} = \frac{1}{M_{z,id}} (1 + 2BM_{w,id}c)^2 \quad (9c)$$

and also

$$\frac{1}{M_{z+1,app}} = \frac{1}{M_{z+1,id}} \frac{(1 + 2BM_{w,id}c)^2}{\left[1 + 2B\left(1 - 3\frac{M_{z,id}}{M_{z+1,id}}\right)M_{w,id}c\right]}. \quad (9d)$$

Eqs. 9 form the basis for the analysis that follows.

### GRAPHICAL METHOD OF ANALYSIS

The method is an extension of a log-log plot first used by Yphantis and Roark (20, 22) to describe the behavior of various "ideal" molecular weight moments. Their method of analyzing a nonideal system involved plotting data as  $\log(M_i)$  vs.  $\log(c)$ , where  $M_i$  is one of the ideal molecular weight moments (e.g.,  $M_{y1}$ ,  $M_{y2}$ ; see Eqs. 14a and b). By direct comparison with standard curves plotted as  $\log(M_i/M_1)$  vs.  $1/(N-1) \log(K_N c^{N-1})$ , they showed that one can obtain, in principle, the stoichiometry, monomer molecular weight, and equilibrium constant for a nonideal system. The novel feature of the method presented here is that by introducing a single dimensionless parameter,  $\beta$ , defined below, one can generate series of standard curves using the ordinary molecular weight averages,  $M_n$ ,  $M_w$ ,  $M_z$ , and  $M_{z+1}$ , which can be employed to get the second virial coefficient as well as the other parameters. The method is extended to treat monomer  $N$ -mer, isodesmic, and type II indefinite self-associating systems, and can also be used to analyze heterogeneous two-species systems (i.e., those that are not in chemical equilibrium) as well as systems composed of both associating and nonassociating monomer  $N$ -mer components. An example of analysis of such a mixed system has appeared (30). The procedure works best if either the monomer molecular weight or stoichiometry or both have been determined previously by some other means, such as a two-species plot (19, 20), or under experimental conditions such that only a single species can be observed.

The reduced ideal molecular weight average ( $M_{i,id}/M_1$ ), where  $i = n, w, z$ , and  $z + 1$  for a monomer  $N$ -mer self-associating system, can be represented as a function of  $\alpha$  in the following way using Eq. 6; letting  $c_1 = (1 - \alpha)c$  and  $c_2 = \alpha c$ , where  $c_1$  and  $c_2$  are the concentration of monomer and  $N$ -mer, respectively,  $\alpha$  is the weight fraction of  $N$ -mer, and  $c$  is the total macromolecular concentration as before:

$$\frac{M_{n,id}}{M_1} = \frac{1}{1 + \left(\frac{1}{N} - 1\right)\alpha} \quad (10a)$$

$$\frac{M_{w,id}}{M_1} = 1 + (N - 1)\alpha \quad (10b)$$

$$\frac{M_{z,\text{id}}}{M_1} = \frac{1 + (N^2 - 1)\alpha}{1 + (N - 1)\alpha} \quad (10\text{c})$$

$$\frac{M_{z+1,\text{id}}}{M_1} = \frac{1 + (N^3 - 1)\alpha}{1 + (N^2 - 1)\alpha} \quad (10\text{d})$$

In addition, we have, from the law of mass action and Eq. 4, that

$$K_N c^{N-1} = \frac{\alpha}{(1 - \alpha)^N}, \quad (11)$$

where  $K_N$  is the equilibrium constant in units of  $(\text{cm}^3/\text{g})^{(N-1)}$  for the self-association reaction

$$nM = P; K_N = \frac{c_N y_N}{c_1^N y_1^N} = \frac{c_N}{c_1^N},$$

where  $M$  and  $P$  represent the monomer and polymer, respectively, and  $n = N$ .

To generate the final relationships to be used for the standard graphs,<sup>2</sup> we combine Eqs. 9–11 to obtain the following equations which are functions only of  $\alpha$ :

$$\frac{M_1}{M_{n,\text{app}}} = 1 + \left(\frac{1}{N} - 1\right)\alpha + \beta \left(\frac{\alpha}{(1 - \alpha)^N}\right)^{1/(N-1)} \quad (12\text{a})$$

$$\frac{M_1}{M_{w,\text{app}}} = \frac{1}{1 + (N - 1)\alpha} + 2\beta \left(\frac{\alpha}{(1 - \alpha)^N}\right)^{1/(N-1)} \quad (12\text{b})$$

$$\frac{M_1}{M_{z,\text{app}}} = \frac{1 + (N - 1)\alpha}{1 + (N^2 - 1)\alpha} \left\{ 1 + 2\beta [1 + (N - 1)\alpha] \left(\frac{\alpha}{(1 - \alpha)^N}\right)^{1/(N-1)\alpha} \right\}^2$$

$$\frac{M_1}{M_{z+1,\text{app}}} = \frac{M_1}{M_{z+1,\text{id}}} \quad (12\text{c})$$

$$\frac{\left[ 1 + 2\beta \left(\frac{M_{w,\text{id}}}{M_1}\right) \left(\frac{\alpha}{(1 - \alpha)^N}\right)^{1/(N-1)} \right]^2}{1 + 2\beta \left[ 1 - 3 \left(\frac{M_{z,\text{id}}}{M_{z+1,\text{id}}}\right) \right] \left(\frac{M_{w,\text{id}}}{M_1}\right) \left(\frac{\alpha}{(1 - \alpha)^N}\right)^{1/(N-1)}}, \quad (12\text{d})$$

where  $\beta$  is defined by

$$\beta = \frac{BM_1}{K_N^{1/(N-1)}} \quad (13)$$

and is a dimensionless parameter reflecting the degree of deviation from ideal behavior for any given extent,  $\alpha$ , of association.

<sup>2</sup>A FORTRAN computer program for generating standard curves is available from the author on request.

In addition to Eqs. 12, we consider three ideal molecular weight moments  $M_{y1}$ ,  $M_{y2}$ , and  $M_{y0}$  (20), which are independent of the second virial coefficient:

$$\frac{M_1}{M_{y1}} = 2 \left[ 1 + \left( \frac{1}{N} - 1 \right) \alpha \right] - \frac{1}{[1 + (N - 1) \alpha]} \quad (14a)$$

$$\frac{M_1}{M_{y2}} = \frac{1 + (N^2 - 1) \alpha}{[1 + (N - 1) \alpha]^3} \quad (14b)$$

$$\frac{M_1}{M_{y0}} = \frac{4[1 + (N - 1) \alpha][1 + (N^2 - 1) \alpha]^3}{\{3[1 + (N^2 - 1) \alpha]^2 - [1 + (N - 1) \alpha][1 + (N^3 - 1) \alpha]\}^2}. \quad (14c)$$

The relationships for  $M_{y1}$  and  $M_{y2}$  will be used in the graphical procedure, while the one for  $M_{y0}$  will be referred to below. The set of theoretical curves to be used for comparison with experimental data is generated by plotting

$$\log (M_{i,app}/M_1) \text{ vs. } \frac{1}{N-1} \log (K_N c^{N-1}) \quad (15)$$

parametrically as functions of  $\alpha$  with  $\beta$  as a parameter expressing nonideality.

Plots of the functions represented by Eqs. 11, 12, and 14 are given in Fig. 1 *a*, *b*, and *c* for monomer-dimer, monomer-trimer, and monomer-tetramer, respectively, for various values of  $\beta$ .

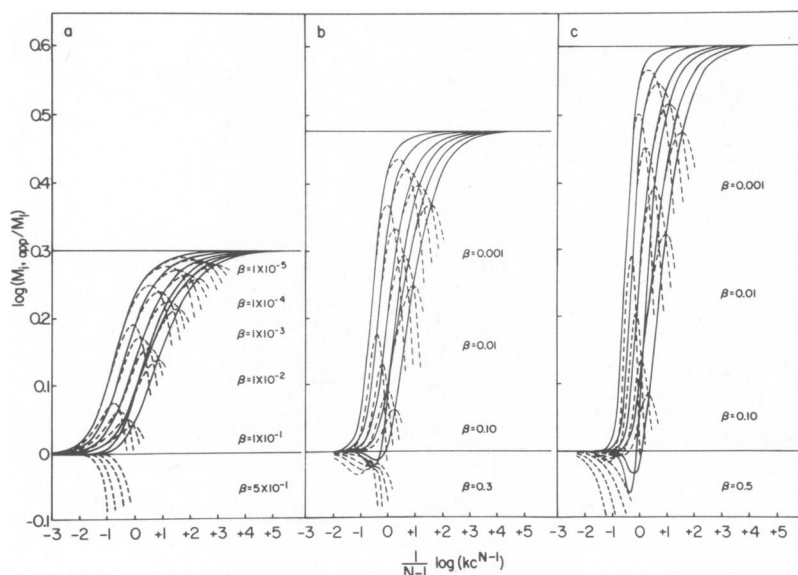


FIGURE 1 Log-log plots for (a) monomer-dimer, (b) monomer-trimer, and (c) monomer-tetramer self-associating systems for various values of  $\beta$  (defined in the text). The solid curves from left to right near the top of each set are, respectively, for  $\beta = 0$ ,  $M_{z+1}$ ,  $M_z$ ,  $M_w$ ,  $M_{y2}$ ,  $M_n$ , and  $M_{y1}$ . Note that the curve for  $M_{y2}$  crosses that for  $M_n$  in the lower region of each set of curves. These standard curves are used to obtain the stoichiometry, monomer molecular weight, equilibrium constant, and second virial coefficient as explained in the text.

The functional dependence of each set of curves (Fig. 1) on  $\log(c)$  is characteristic of the stoichiometry and is used by comparison with experimental data to determine the stoichiometry of association. For weakly associating systems the shape of the  $\log(M_{y1}/M_1)$  and  $\log(M_{y2}/M_1)$  curves is quite characteristic of the stoichiometry and can be used as a diagnostic feature if sufficiently precise data have been obtained (20).

## ESTIMATION OF EQUILIBRIUM CONSTANT AND SECOND VIRIAL COEFFICIENT

### *Moderately Nonideal Systems; $\beta < 0.1$*

The data are plotted as  $\log(M_{i,app})$  vs.  $\log(c)$  on the same scale as the standard graphs and, if  $M_1$  is known, the plots of  $\log(M_{y1})$  and  $\log(M_{y2})$  and the lower parts of  $\log(M_{z+1})$ ,  $\log(M_z)$ ,  $\log(M_w)$ , and  $\log(M_n)$  are superimposed on the standard plots and the equilibrium constant is taken from the intercept of the origin of the abscissa of the experimental plot on the abscissa of the standard plot. In addition, if  $M_1$  is to be estimated, the intercept of the origin of the ordinate of the theoretical plot with the ordinate of the experimental plot will give  $\log(M_1)$ . The second virial coefficient can be estimated by comparing the data with curves with various values of  $\beta$ . A procedure for obtaining both  $\beta$  and  $K_N$  from the maximum, if such a maximum is observed, in the  $\log(M_{i,app})$  curves is given below, and is useful for determining values of  $\beta$  used to generate standard curves.

### *Strongly Nonideal Systems; $\beta > 0.1$*

The best way to obtain  $\beta$  for a strongly nonideal system is to obtain first a value of  $K_N$  from the  $x$ -axis intercept using  $M_{y1}$  and  $M_{y2}$  and then at a particular value of  $\alpha$  to make successive guesses at  $\beta$  using Eqs. 12 until the  $\log(M_{i,app}/M_1)$  calculated agree with those observed. Then a set of theoretical curves is generated using this value of  $\beta$  to see if agreement is observed over the entire span of data. This procedure is repeated at several values of  $\alpha$ , readjusting  $K_N$  or choosing another value of  $N$ , if necessary, until a satisfactory fit is obtained.

## ISODESMIC INDEFINITE SELF-ASSOCIATION

An isodesmic indefinite self-association is one of indefinite extent whose successive molar equilibrium constants are equal (5, 6, 31–33). For a self-association of this type we have

$$\frac{M_{n,id}}{M_1} = \frac{1 + (1 + 4\gamma)^{1/2}}{2} \quad (16a)$$

$$\frac{M_{w,id}}{M_1} = 1 + (1 + 4\gamma)^{1/2} \quad (16b)$$

$$\frac{M_{z,id}}{M_1} = \frac{(1 + 6\gamma)}{(1 + 4\gamma)^{1/2}} \quad (16c)$$

In addition, since  $M_{z+1} = [d(cM_w M_z)]/[d(cM_w)]$  we also have

$$\frac{M_{z+1,id}}{M_1} = \frac{(1 + 12\gamma)(1 + 4\gamma)^{1/2}}{(1 + 6\gamma)}, \quad (16d)$$

where  $\gamma = kc$  and  $k$  is the equilibrium constant for the addition of successive monomers in units of (cm<sup>3</sup>/g). For a nonideal isodesmic system the following relations apply from Eqs. 9 a–d:

$$\frac{M_1}{M_{n,app}} = \frac{2}{1 + (1 + 4\gamma)^{1/2}} + \beta\gamma \quad (17a)$$

$$\frac{M_1}{M_{w,app}} = \frac{1}{(1 + 4\gamma)^{1/2}} + 2\beta\gamma \quad (17b)$$

$$\frac{M_1}{M_{z,app}} = \frac{(1 + 4\gamma)^{1/2}}{(1 + 6\gamma)} [1 + 2\beta(1 + 4\gamma)^{1/2}\gamma]^2 \quad (17c)$$

$$\frac{M_1}{M_{z+1,app}} = \frac{M_1}{M_{z+1,id}} \frac{\left[1 + 2\beta\left(\frac{M_{w,id}}{M_1}\right)\gamma\right]^2}{\left\{1 + 2\beta\left[1 - 3\left(\frac{M_{z,id}}{M_{z+1,id}}\right)\right]\left(\frac{M_{w,id}}{M_1}\right)\gamma\right\}}, \quad (17d)$$

where  $\beta$  is a dimensionless parameter defined by

$$\beta \equiv \frac{BM_1}{k}. \quad (18)$$

Finally, for a system whose nonideality is restricted to the second virial coefficient, we have the ideal molecular weight moments as above.

$$\frac{M_1}{M_{y1}} = \frac{4}{1 + (1 + 4\gamma)^{1/2}} - \frac{1}{(1 + 4\gamma)^{1/2}} \quad (19a)$$

$$\frac{M_1}{M_{y2}} = \frac{(1 + 6\gamma)}{(1 + 4\gamma)^{3/2}} \quad (19b)$$

$$\frac{M_1}{M_{y0}} = \frac{(1 + 4\gamma)^{1/2}}{(1 + 6\gamma)} \left[ \frac{3}{2} - \frac{(1 + 12\gamma)(1 + 4\gamma)}{2(1 + 6\gamma)^2} \right]^{-2}. \quad (19c)$$

Again, theoretical curves can be generated by plotting  $\log(M_{i,app}/M_1)$  vs.  $\log(\gamma)$ , with  $\beta$  as a parameter expressing nonideality. Curves for various values of  $\beta$  are presented in Fig. 2. Experimental data are plotted as  $\log(M_{i,app})$  vs.  $\log c$ , superimposed on the theoretical curves, and the intercepts of the axes used to obtain  $\log(k)$  and  $\log(M_1)$  as explained above for monomer  $N$ -mer systems. The second virial coefficient is also obtained as explained above.

## TYPE II INDEFINITE SELF-ASSOCIATING SYSTEMS

Another type of indefinite self-association that can be treated by the methods described here is the so-called type II indefinite self-association in which only monomer and even ( $N = 2i$ ;  $i = 1, 2, 3, 4 \dots$ ) polymers are present. A simple expression for the apparent molecular weight moments as a function of total concentration cannot be written, but both the moments and total concentration can be expressed as parametric functions of the monomer concentration (33). One can plot  $\log(M_i/M_1)$  vs.  $\log(kc)$  with  $\beta = BM_1/k$  as a parameter as above.



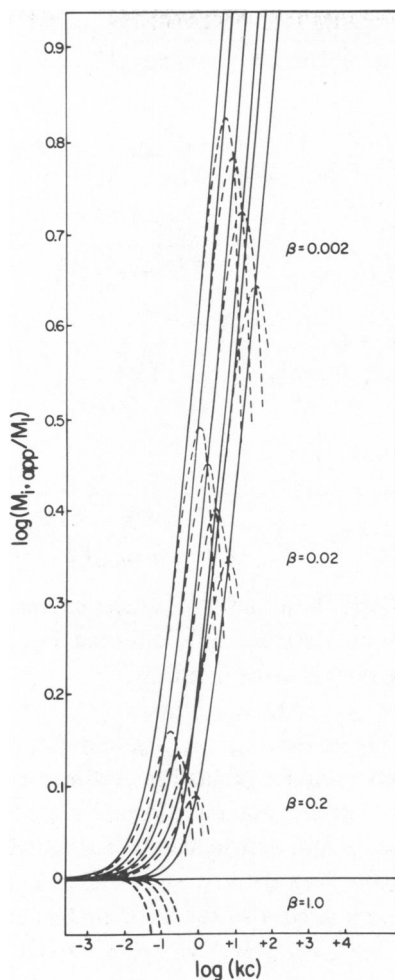


FIGURE 2 Log-log plots for an isodesmic indefinite self-associating system for various values of  $\beta$  (defined in text). The curves are as explained in the legend to Fig. 1.

#### DETERMINATION OF $BM_1$ AND $K_N$ FROM THE MAXIMUM

If a range of concentrations has been chosen such that a maximum is observed in a graph of  $M_{n,app}$ ,  $M_{w,app}$ , or  $M_{z,app}$  vs.  $c$  for a monomer  $N$ -mer self-associating system, then the following relationships are useful for analysis of the system:

$$\frac{M_{n,app,max}}{M_1} = \frac{[1 + (N - 1)\alpha_{max,n}]}{[1 + 2 \frac{(N - 1)^2}{N} \alpha_{max,n}(1 - \alpha_{max,n})]} \quad (20a)$$

$$\frac{M_{w,app,max}}{M_1} = \frac{[1 + (N - 1)\alpha_{max,w}]^3}{[1 + (N^2 - 1)\alpha_{max,w}]} \quad (20b)$$

$$\frac{M_{z,app,max}}{M_1} = \frac{\{3[1 + (N^2 - 1)\alpha_{max,z}]^2 - [1 + (N - 1)\alpha_{max,z}][1 + (N^3 - 1)\alpha_{max,z}]\}^2}{4[1 + (N - 1)\alpha_{max,z}][1 + (N^2 - 1)\alpha_{max,z}]^3} \quad (20c)$$

$$\beta_n = \frac{(N - 1)^2}{N} \frac{(1 - \alpha_{max,n})^{N+1}}{[1 + (N - 1)\alpha_{max,n}]} \left[ \frac{\alpha_{max,n}}{(1 - \alpha_{max,n})^N} \right]^{(N-2)/(N-1)} \quad (21a)$$

$$\beta_w = \frac{(N - 1)^2}{2} \frac{(1 - \alpha_{max,w})^{N+1}}{[1 + (N - 1)\alpha_{max,w}]^3} \left[ \frac{\alpha_{max,w}}{(1 - \alpha_{max,w})^N} \right]^{(N-2)/(N-1)} \quad (21b)$$

$$\beta_z = \frac{N(N + 1)}{2[1 + (N - 1)\alpha_{max,z}]} \left[ \frac{\alpha_{max,z}}{(1 - \alpha_{max,z})^N} \right]^{1/(N-1)} \cdot \frac{1}{\left\{ 2[1 + (N^2 - 1)\alpha_{max,z}] \left[ (N - 1) + \frac{[1 + (N - 1)\alpha_{max,z}]^2}{(N - 1)\alpha_{max,z}(1 - \alpha_{max,z})} \right] - N(N - 1) \right\}}, \quad (21c)$$

where  $\alpha_{max,n}$ ,  $\alpha_{max,w}$ , and  $\alpha_{max,z}$  are the values of  $\alpha$  at the maximum in graphs of  $M_{n,app}$ ,  $M_{z,app}$ , and  $M_{z,app}$  vs.  $c$ . Eqs. 21 were obtained by differentiating Eqs. 12 with respect to  $\alpha$ . Eqs. 20 were obtained by substituting Eqs. 21 back into Eqs. 12.

After obtaining values of  $M_{n,app,max}$ ,  $M_{w,app,max}$ , and  $M_{z,app,max}$  from the graph of  $M_{n,app}$ ,  $M_{w,app}$ , and  $M_{z,app}$  vs.  $c$ , one obtains values for  $\alpha_{max,n}$ ,  $\alpha_{max,w}$ , and  $\alpha_{max,z}$  by successive approximations from Eqs. 12a, b, and c after a value for  $N$  has been estimated. These values of  $\alpha_{max,n}$ ,  $\alpha_{max,w}$ , and  $\alpha_{max,z}$  and the values of  $c$  at the maximum can be substituted into Eq. 11 to obtain estimates of  $K_N$ . The virial coefficient, in turn, can be estimated from Eq. 13. The parameters can also be estimated graphically (Fig. 3). Error estimates are given in Fig. 3 c.

Both  $BM_1$  and  $k$  can be estimated also for isodesmic self-associating systems from the positions of the maxima in  $\log (M_{i,app}/M_1)$  vs.  $\log (c)$  plots. The following relations are employed similarly to those for the monomer  $N$ -mer case above:

$$\frac{M_{n,app,max}}{M_1} = \frac{[1 + (1 + 4\gamma_{max,n})^{1/2}](1 + 4\gamma_{max,n})^{1/2}}{3(1 + 4\gamma_{max,n})^{1/2} - 1} \quad (22a)$$

$$\frac{M_{w,app,max}}{M_1} = \frac{(1 + 4\gamma_{max,w})^{3/2}}{(1 + 6\gamma_{max,w})} \quad (22b)$$

$$\frac{M_{z,app,max}}{M_1} = \frac{(1 + 10\gamma_{max,z} + 30\gamma_{max,z}^2)^2}{(1 + 4\gamma_{max,z})^{1/2}(1 + 6\gamma_{max,z})^3} \quad (22c)$$

$$\beta_n = \frac{4}{(1 + 4\gamma_{max,n})^{1/2}[1 + (1 + 4\gamma_{max,n})^{1/2}]^2} \quad (23a)$$

$$\beta_w = \frac{1}{(1 + 4\gamma_{max,w})^{3/2}} \quad (23b)$$

$$\beta_z = \frac{(1 + 3\gamma_{max,z})}{(1 + 4\gamma_{max,z})^{1/2}(1 + 10\gamma_{max,z} + 30\gamma_{max,z}^2)} \quad (23c)$$

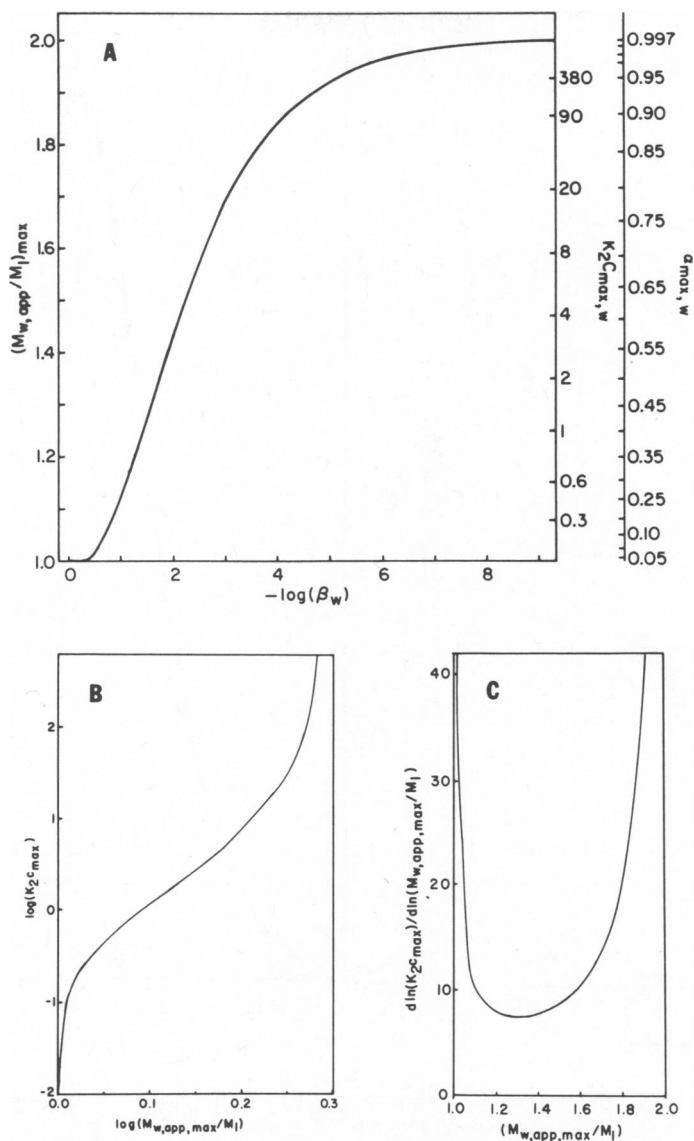


FIGURE 3 Monomer-dimer systems, shown to emphasize the single-valued relationship between  $K_2c_{max}$ ,  $\beta_w$ , and  $(M_{w,app,max}/M_1)$ . (a) Graph of  $(M_{w,app,max}/M_1)$  vs.  $-\log(\beta_w)$ , used to obtain  $\beta_w$ , with  $K_2c_{max}$  and  $\alpha_{max,w}$  as the right-hand ordinates. (b) Graph of  $\log(K_2c_{max})$  vs.  $\log(M_{w,app,max}/M_1)$  used to obtain  $K_2$ . (c) Graph of the percentage error in  $K_2c_{max}$  for a 1% error in  $(M_{w,app,max}/M_1)$  as a function of  $(M_{w,app,max}/M_1)$  showing that the useful range of this method is roughly  $1.1 \leq (M_{w,app,max}/M_1) \leq 1.8$ .

## TESTS OF THE GRAPHICAL METHOD

The methods presented above have been tested on data for several systems presented in the literature. Both the graphical (log-log) method and the method for obtaining the equilibrium constant and second virial coefficient from the maximum gave results in good agreement with those reported. Two examples of the graphical method are given, one for nonideal monomer-

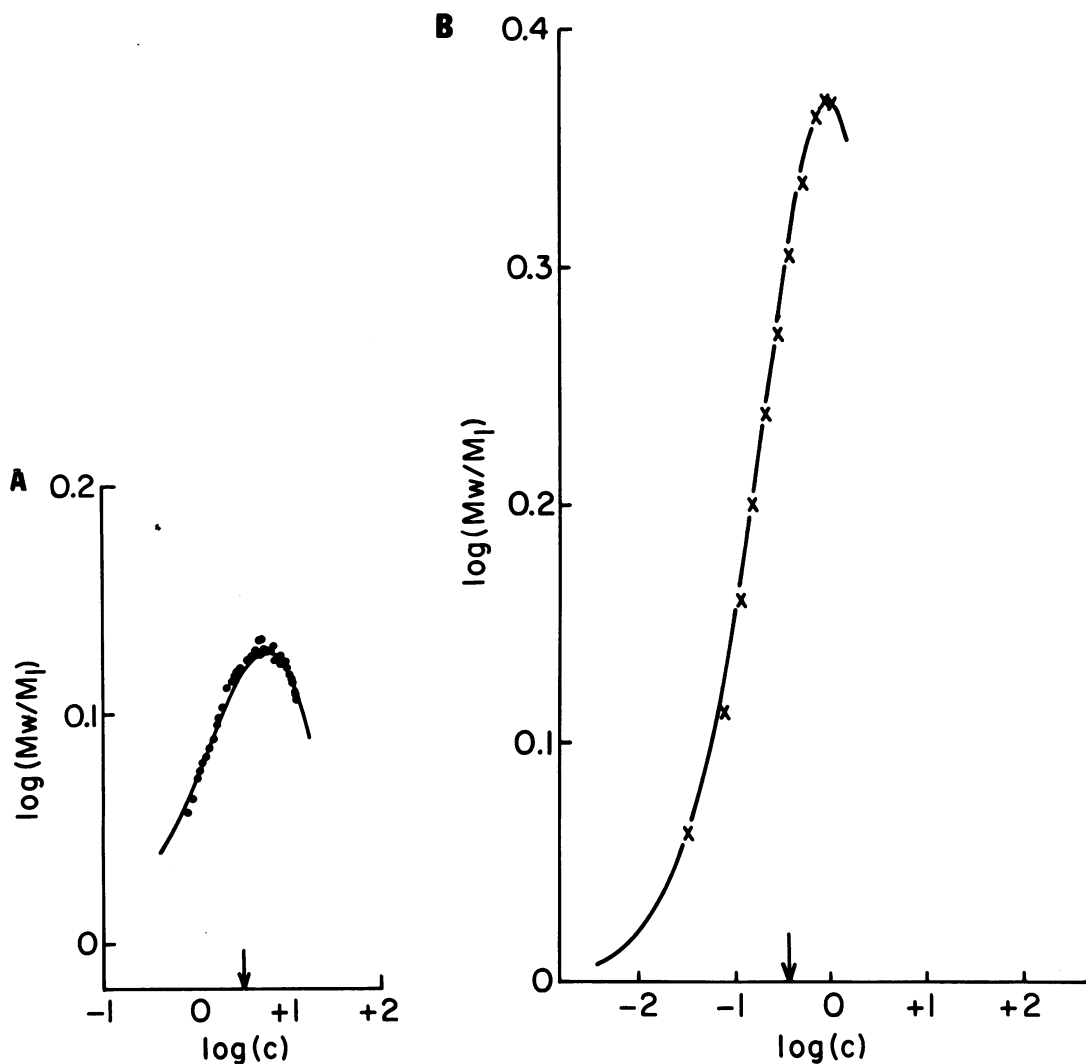


FIGURE 4 (A) Log-log plot of data for the monomer-dimer self-association of  $\beta$ -lactoglobulin A;  $\Gamma/2 = 0.10$ , pH 2.46, at 20°C from the work of Tang (34). A value of  $\beta_w = 0.0195$  was estimated from the maximum value of  $M_{w,app}/M_1$ . A value of  $K_2 = 3.2$  dl/g was obtained from the x-axis intercept and agrees well with the value of 3.5 dl/g reported by him. A value of  $BM_1 = 0.062$  dl/g was obtained from the product  $\beta K_2$  and also agrees with the value of 0.067 dl/g reported by him. (B) Log-log plot of data for the isodesmic indefinite self-association of purine taken from Van Holde and Rossetti (5). The points were taken from an interpolation curve drawn through their data. A value of  $\beta_w = 0.025$  used for the plot was taken from the maximum value of  $M_{w,app}/M_1$ . A value of  $k = 2.97$  M<sup>-1</sup> was obtained from the x-axis intercept and agrees well with their value of 2.80 M<sup>-1</sup>. A value of  $BM_1 = 0.074$  M<sup>-1</sup> was obtained from the product  $\beta k$  and agrees well with their reported value of 0.074 M<sup>-1</sup>.

dimer self-association of  $\beta$ -lactoglobulin A at pH 2.46 (34), the other for the nonideal isodesmic indefinite self-association of purine (5). The graphical analyses of both systems are shown in Fig. 4, while the result obtained from the use of the maximum in the plots is given in Table I. Also included in Table I are results obtained with the maximum method (Eqs. 20–23) for several other systems reported. These relationships will give values of the equilibrium

TABLE I  
COMPARISON OF VALUES OF  $K$  AND  $BM_1$  ESTIMATED FROM THE MAXIMUM WITH  
VALUES REPORTED IN THE LITERATURE

System	Reference	$(M_{w,app}/M_1)_{\max}$	$\alpha_{\max}$	$\beta$	$c_{\max}$	Reported in reference		Calculated from maximum	
						$K$	$BM_1$	$K$	$BM_1$
purine*	5	2.36	2.71‡	$2.5 \times 10^{-2}$	0.91 M	$2.80 \text{ M}^{-1}$	$0.074 \text{ M}^{-1}$	$2.97 \text{ M}^{-1}$	$0.074 \text{ M}^{-1}$
$\beta$ -lactoglobulin B pH 2.58, $T/2 = 0.10$ $t = 25^\circ\text{C}$	45	1.38	0.53	$1.45 \times 10^{-2}$	0.45 g/dl	4.25 dl/g	0.108 dl/g	5.28 dl/g	0.078 dl/g
$\beta$ -lactoglobulin A pH 2.46, $T/2 = 0.10$ $t = 20^\circ\text{C}$	34	1.34	0.49	$1.95 \times 10^{-2}$	0.56	3.50	0.067	3.2	0.062
$\beta$ -lactoglobulin B pH 2.64, $T/2 = 0.16$ $t = 25^\circ\text{C}$	46	1.56	0.68	$3.46 \times 10^{-3}$	0.32	23.1	0.055	20.8	0.072
myosin rod	47	1.12	0.26	$1.01 \times 10^{-1}$	0.06	8.0	0.84	7.9	0.80
myosin rod	47	1.10§	0.35	$1.00 \times 10^{-1}$	0.10	8.0	0.84	8.3	0.83
light meromyosin	47	1.17	0.46	$5.34 \times 10^{-2}$	0.18	10	0.52	8.8	0.47
myosin	48	1.08	0.20	$1.50 \times 10^{-1}$	0.035	8.9	1.3	10.0	1.5
$\beta$ -lactoglobulin C $T/2 = 0.10$ , $t = 25^\circ\text{C}$	49	1.42	0.56	$1.12 \times 10^{-2}$	0.34	5.9	0.123	8.5	0.095
histone tetramer	50	1.45	0.59	$8.57 \times 10^{-3}$	0.43	0.68	0.007	0.81	0.0068

t, temperature.

\*Purine self-association is isodesmic; the other systems reported in this table are monomer-dimer.

‡ $kc_{\max}$

§ $(M_{n,app}/M_1)_{\max}$ , taken from the point  $M_{w,app} = M_{n,app}$ . See Eq. 24a.

|| $(M_{w,app}/M_1)_{\max}$  was taken from the point  $M_{z,app} = M_{w,app}$ . See Eq. 24b.

constant consistent with that obtained from the  $x$ -axis intercept of the log-log plots if the correct monomer molecular weight and mode of association have been determined. Therefore, they serve as a useful check on the conclusions reached by other methods.

## NOTABLE FEATURES AND PRECAUTIONS

It is interesting to note that at  $C_{\max, n}$

$$\frac{M_1}{M_{n,app,\max}} = \frac{M_1}{M_{y1}} = \frac{M_1}{M_{w,app}}, \quad (24a)$$

at  $C_{\max, w}$

$$\frac{M_1}{M_{w,app,\max}} = \frac{M_1}{M_{y2}} = \frac{M_1}{M_{z,app}}, \quad (24b)$$

and at  $C_{\max, z}$

$$\frac{M_1}{M_{z,app,\max}} = \frac{M_1}{M_{y0}} = \frac{M_1}{M_{z+l,app}}, \quad (24c)$$

for both monomer  $N$ -mer and isodesmic self-associating systems. The first half of these relationships can be obtained by comparing the monomer  $N$ -mer relationships (Eqs. 12) with Eqs. 14, and the isodesmic relationships (Eqs. 17) with Eqs. 19. The second half follows from the definition for  $M_{y1}$ ,  $M_{y2}$ , and  $M_{y0}$  (18). In fact, Eqs. 24 can be shown to hold at any extremum, either a maximum or a minimum, and are not necessarily characteristic of the

mode of association or extent of nonideality. Therefore, one should use the complete set of molecular weight moments and compare the relative heights and positions of their respective maxima to see that they are self-consistent, since systematic errors in the data caused by a bad blank correction, incorrect focus, or excessively noisy data could lead to fluctuations in the moments that might be interpreted as nonideal self-association.

Curves for various values of  $\beta$  (Figs. 1 and 2) have been truncated just after the maxima for the sake of clarity. Obviously, there could exist systems for which the entire observable extent of the data would lie to the right of the maxima. Systems of this type could be mistaken for anomalously behaving nonideal systems composed of a single species, unless several molecular weight averages were used. Extrapolation from such regions of data on the customary plot of  $1/M_w$  vs.  $c$  might suggest the need for more than one virial coefficient to describe the data and would give an erroneous value for the infinite dilution value of the molecular weight of the presumed species. Fig. 5 shows a nonideal monomer-dimer system with a value of 0.01 for  $\beta$ . The inverse reduced weight average molecular weight is plotted vs.  $K_2c$  for values of  $0.7 \leq \alpha \leq 0.91$ , for which the deviation from linearity is no more than 2%. Use of the ideal molecular weight moments and other of the ordinary moments would be necessary for the correct analysis of this system. Furthermore, it should be pointed out that the limiting slope as  $c \rightarrow 0$  in Fig. 5 gives neither the quantity  $(2BM_1 - K_2)$  nor any other parameter relevant to the analysis of the system. Generally, procedures using such a limiting slope procedure are not applicable unless the weight fraction of the dimer does not exceed 0.07 over the range of data used to estimate the slope, since the power series expansion of  $1/M_w$  vs.  $c$  for a monomer-dimer system has a linear range which at best extends to 7% association (26).

The graphical method works best for data spanning from about  $\alpha \leq 0.25$  to  $\geq 0.80$  if stoichiometry,  $M_1$ , and equilibrium constant are to be estimated. On the other hand, if the stoichiometry and  $M_1$  are known, then only a relatively short span of data is required to get the

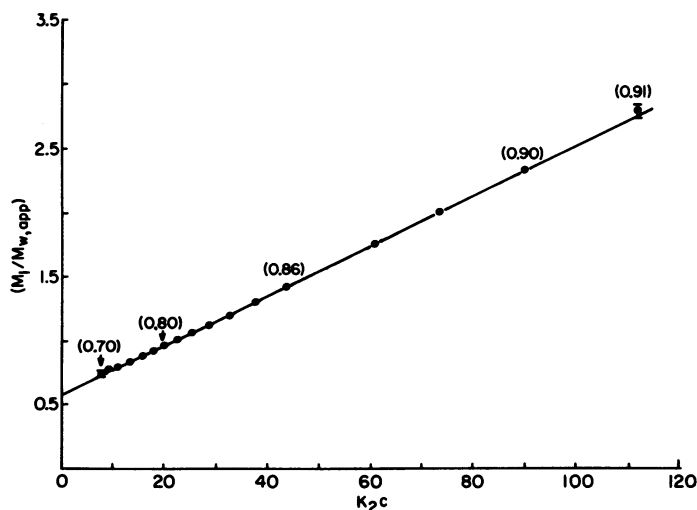


FIGURE 5 Graph of  $(M_1/M_{w,app})$  vs.  $K_2c$  for  $\beta = 0.01$ . See text for explanation. Values of  $\alpha$  are shown in parentheses.

equilibrium constant for both ideal and nonideal systems. The most accurate estimate of parameters for nonideal systems can be obtained for those systems that exhibit maxima in the plots of  $M_{i,app}$  vs.  $c$ .

Difficulties in the analysis may arise from at least four basic sources: (a) incorrect choice of a model because of ambiguous data, (b) systematic errors in the computation of the moments, (c) systematic errors from poor blank correction, or (d) large random errors in the primary data. One may often find that the choice of a model is arbitrary because two or more models fit the data nearly equally well. Such cases may arise especially in systems for which either the monomer molecular weight or stoichiometry is not known accurately. For example, the  $M_w(r)$  for purine isodesmic self-association (Fig. 4 B) can be fitted with nearly the same precision to a monomer-trimer model with  $\beta = 5.44 \times 10^{-3}$  and an estimate of  $M_1$  that is 10% higher than the true value. However, this ambiguity could be resolved if more data were collected at higher concentrations and if other moments such as  $M_z(r)$  and  $M_{y2}(r)$  were employed. The maximum in the monomer-trimer standard curve is considerably broader than the one for the isodesmic model. This difference would become apparent at higher concentrations, leading to rejection of the monomer-trimer model. If, on the other hand, the correct, isodesmic model were chosen for the purine case, a 10% error in  $M_1$  would lead to only a  $\sim 10\%$  error in  $BM_1$  and a  $\sim 25\%$  error in  $k$ , with fits noticeably poorer than with the correct molecular weight. A classic example of an ambiguous case is lysozyme (13,35), which can be fit to either a nonideal monomer-dimer or a slightly more nonideal isodesmic model. Again, this ambiguity could be resolved if observations were made at a higher concentrations such that  $M_w/M_1 > 1.25$  and if other moments in addition to  $M_w(r)$  were employed. Any method of analysis will fail if the data do not span a concentration range that provides unambiguous information.

Systematic errors in the computation of  $M_w(r)$  and  $M_n(r)$ , which are also reflected strongly in  $M_{y1}(r)$  and  $M_{y2}(r)$ , will lead to characteristic inconsistencies in the set of log-log plots such that no model can be fit. These errors arise from the choice of the zero level of concentration and from the estimation of an integration constant needed to compute  $M_n(r)$ , and can be reduced by choosing rotor speeds that effect meniscus depletion (25). It is recommended that one start the analysis using  $M_z(r)$ , since its estimation is not dependent on choices of either of these constants. One first chooses a model using  $M_z(r)$  alone and if necessary makes various choices for zero level, recomputing the moments until a self-consistent set of curves is found. If a set of self-consistent curves cannot be found by this method, one may assume that the model is wrong. This practice is not recommended, however, unless the monomer molecular weight is known accurately.

Random errors in the primary  $c$  vs.  $r$  data will lead to fluctuations in the moments.  $M_{z+1}$  is the most sensitive to noise and cannot be estimated reliably in many cases. The other moments can be estimated with a precision of 2–3% in  $M_w$ , 5% in  $M_z$ , 5–10% in  $M_n$ ,  $M_{y1}$ , and  $M_{y2}$ . In practice, large random errors ( $\geq \pm 0.005$  mm) often lead also to incorrect choices in the zero level and integration constant, introducing systematic errors into the moments depending on them. It is recommended that laser optics (36–39), fine grain films, and automated plate reading equipment (30, 40–43) be employed to collect fringe displacement data. Primary data with random errors of  $\pm 0.002$  mm or less can be obtained routinely with such equipment. The moments of the distribution should be estimated with one of the standard computer programs developed for this purpose. This author has had most experience with the one developed by

Roark and Yphantis (20) and finds it adequate in most cases to do this type of analysis. This program allows input of the meniscus concentration, if necessary, and uses several methods to compute the integration constant for  $M_n(r)$ , depending on what is known about the system.

It is worth pointing out that nonideal behavior of two-species plots also can be treated through the dimensionless parameter,  $\beta$ . As for the other plots above, deviation from ideality is dependent only on the value of  $\beta$ .

## CONCLUSION

A graphical procedure for the analysis of nonideal monomer  $N$ -mer, isodesmic, and type II indefinite self-associating systems has been described. The procedure is especially useful for analysis of monomer-trimer and higher monomer  $N$ -mer self-associations for which simple analytical expressions do not exist. By comparing the concentration-dependent behavior of the ordinary molecular weight averages,  $M_n$ ,  $M_w$ ,  $M_z$ , and  $M_{z+1}$  with standard curves for various self-association schemes, one can determine a dimensionless parameter,  $\beta$ , defined above, which characterizes the nonideal behavior of the system as long as the logarithm of the activity coefficient of the macromolecular species can be represented as a linear function of the total macromolecular concentration (see Eq. 4). In principle, one can obtain from these plots the stoichiometry, monomer molecular weight, equilibrium constant, and second virial coefficient. An account of the procedures described here was presented at the 1979 meeting of the Biophysical Society (44).

The basic principles involved here can be extended to treat ideal three-species, type III, and type IV indefinite self-associating systems using the ordinary molecular weight moments, and nonideal three species, type III, and type IV indefinite self-associating systems using the ideal moments. In principle, the method can be extended to treat monomer  $N$ -mer, isodesmic, and type II indefinite self-associating systems with nonideality appearing in either the second and third or second and fourth virial coefficients if the ideal moments are employed. Fundamentally, if the stoichiometry and monomer molecular weight are known, these are all two-parameter systems. After an equilibrium constant has been estimated from the  $x$ -axis intercept, the second parameter may be estimated by comparison of the data with standard curves generated for various values of the second parameter. If the concentration span is sufficient, the two parameters will be uniquely determined, in principle.

The methods described are not restricted to data obtained by ultracentrifugation and can be used directly for analysis of thermodynamically homogeneous, single-component, self-associating systems by osmotic pressure and light-scattering measurements.

I thank Nancy O'Donoghue for preparing the figures and Bill Saunders for photographing them.

This work was supported by grant HL-21488 from the National Institutes of Health.

Received for publication 5 April 1979 and in revised form 20 August 1979.

## REFERENCES

1. TISELIUS, A. 1962. Über die Berechnung thermodynamischer Eigenschaften von Kolloiden Lösungen aus Messungen mit der Ultrazentrifuge. *Z. Phys. Chem.* **124**:449.
2. RAO, M. S. N., and G. KEGELES. 1958. An ultracentrifuge study of the polymerization of  $\alpha$ -chymotrypsin. *J. Am. Chem. Soc.* **80**:5724.



3. SQUIRE, P. G., and C. H. LI. 1961. Adrenocorticotropin (ACTH). XXIII. A sedimentation study of the state of aggregation of ovine pituitary ACTH in acidic and basic solutions. *J. Am. Chem. Soc.* **83**:3521.
4. ADAMS, E. T., JR. and H. FUJITA. 1963. Sedimentation equilibrium in reacting systems. In *Ultracentrifugation Analysis in Theory and Experiment*. J. W. Williams, editor. Academic Press, Inc., New York. 119.
5. VAN HOLDE, K. E., and G. P. ROSSETTI. 1967. A sedimentation equilibrium study of the association of purine in aqueous solutions. *Biochemistry*. **6**:2189.
6. ADAMS, E. T. JR. 1967. Analysis of self-associating systems by sedimentation equilibrium experiments. *Fractions*. Beckman Instruments, Palo Alto, Calif. No. 3, 1.
7. YPHANTIS, D. A., editor. 1969. Advances in ultracentrifugal analysis. *Ann. N. Y. Acad. Sci.* **164**:1.
8. WILLIAMS, J. W. 1972. Ultracentrifugation of Macromolecules. Modern Topics. Academic Press, Inc., New York.
9. TELLER, D. C. 1973. Characterization of proteins by sedimentation equilibrium in the analytical ultracentrifuge. *Methods enzymol.* **27D**:346.
10. VAN HOLDE, K. E. 1975. Sedimentation analysis of proteins. In *The Proteins*. H. Neurath, R. L. Hill, and C. Boeder, editors. Academic Press, Inc., New York. Vol I. 3rd ed. 256.
11. FUJITA, H. 1975. Foundations of Ultracentrifugal Analysis. John Wiley & Sons, Inc., New York.
12. LEWIS, M. S., and G. H. WEISS, editors. 1976. Proceedings of the conference fifty years of the ultracentrifuge. *Biophys. Chem.* **5**:1.
13. EISENBERG, H. 1976. Biological Macromolecules and Polyelectrolytes in Solution. Oxford University Press, Inc. Oxford.
14. KIM, H., R. C. DEONIER, and J. W. WILLIAMS. 1977. The investigation of self-association reactions by equilibrium ultracentrifugation. *Chem. Rev.* **11**:659.
15. HASCHEMEYER, R. H., and W. F. BOWERS. 1970. Exponential analysis of concentration or concentration difference data for discrete molecular weight distributions in sedimentation equilibrium. *Biochemistry*. **9**:435.
16. YPHANTIS, D. A., M. L. JOHNSON, and G. M. WU. 1972. Effect and detection of heterogeneity in self-associating systems. *Am. Chem. Soc.* **163**:2. (Abstr.).
17. CHUN, P. W., and J. S. KIM. 1975. Determination of the equilibrium constants of self-associating protein systems. *Biophys. Chem.* **3**:46.
18. MILTHORPE, B. K., P. D. JEFFERY, and L. W. NICHOL. 1975. The direct analysis of sedimentation equilibrium results obtained with polymerizing systems. *Biophys. Chem.* **3**:169.
19. SOPHIANOPOULOS, A. J. and K. E. VAN HOLDE. 1964. Physical studies of muramidase (lysozyme) II, pH dependent dimerization. *J. Biol. Chem.* **239**:2516.
20. ROARK, D. E., and D. A. YPHANTIS. 1969. Studies of self-associating systems by equilibrium ultracentrifugation. *Ann. N. Y. Acad. Sci.* **164**:245.
21. CHUN, P. W., and J. S. KIM. 1970. Determination of equilibrium constants of associating protein systems. Graphical analysis for discrete and indefinite associations. *Biochemistry*. **9**:1951.
22. YPHANTIS, D. A., and D. E. ROARK. 1972. Equilibrium centrifugation of non-ideal systems. Molecular weight moments for removing the effects of non-ideality. *Biochemistry*. **11**:2925.
23. CHUN, P. W., J. S. KIM, J. D. WILLIAMS, W. T. COPE, L. H. TANG, and E. T. ADAMS, JR. 1972. Graphical approach to non-ideal cases of self-associating protein systems. *Biopolymers*. **11**:197.
24. GOLDBERG, R. J. 1953. Sedimentation in the ultracentrifuge. *J. Phys. Chem.* **57**:194.
25. YPHANTIS, D. A. 1964. Equilibrium ultracentrifugation of dilute solutions. *Biochemistry*. **3**:297.
26. STAFFORD, W. F., III, and D. A. YPHANTIS. 1972. Virial expansions for ideal self-associating systems. *Biophys. J.* **12**:1359.
27. ROARK, D. E., and D. A. YPHANTIS. 1971. Equilibrium centrifugation of non-ideal systems. The Donnan effect in self-associating systems. *Biochemistry*. **10**:3241.
28. TANFORD, D. 1961. Physical Chemistry of Macromolecules. John Wiley & Sons, Inc., New York. 000.
29. LANSING, W. D., and E. O. KRAEMER. 1935. Molecular weight analysis of mixtures by sedimentation equilibrium in the Svedberg ultracentrifuge. *J. Am. Chem. Soc.* **57**:1369.
30. POLLARD, T. D., W. F. STAFFORD, III, and M. E. PORTER. 1978. Characterization of a second myosin from *Acanthamoeba castellanii*. *J. Biol. Chem.* **253**:4798.
31. ELIAS, H. G., and R. BAREISS. 1967. Assoziation von Makromolekülen. *Chimia*. **12**:53.
32. VAN HOLDE, K. E., G. P. ROSSETTI, and R. D. DYSON. 1969. Sedimentation equilibrium of low-molecular weight associating solutes. *Ann. N.Y. Acad. Sci.* **164**:279.
33. TANG, L. H., D. R. POWELL, B. M. ESCOTT, and E. T. ADAMS, JR. 1977. Analysis of various indefinite self-associations. *Biophys. Chem.* **7**:121.
34. TANG, L. H. 1971. Sedimentation equilibrium studies on beta-lactoglobulin A at acid pH's. Ph.D. Dissertation. Illinois Institute of Technology, Chicago, Ill.

35. DEONIER, R. C., and J. W. WILLIAMS. 1970. Self association of muramidase (lysozyme) in solution at 25°, pH 7.0 and I = 0.20. *Biochemistry*. **9**:4260.
36. WILLIAMS, R. C., JR. 1972. A laser light source for the analytical ultracentrifuge. *Anal. Biochem.* **48**:164.
37. WILLIAMS, R. C., JR. 1978. Continuous laser optics in the ultracentrifuge. *Methods Enzymol.* **48F**:185.
38. LEWIS, J. A., and J. W. LYTTLETON. 1973. An optical pulse modulation system for laser interference studies in the ultracentrifuge. *Anal. Biochem.* **56**:52.
39. PAUL, C. H., and D. A. YPHANTIS. 1972. Pulsed laser interferometry (PLI) in the analytical ultracentrifuge. I. Systems Design. *Anal. Biochem.* **48**:588.
40. DEROSIER, D. J., P. MUNK, and D. J. COX. 1972. Automatic measurement of interference photographs from the ultracentrifuge. *Anal. Biochem.* **50**:139.
41. CARLISLE, R. M., J. I. H. PATTERSON, and D. E. ROARK. 1974. An automated microcomparator for ultracentrifuge interference fringe measurements. *Anal. Biochem.* **61**:248.
42. MARGOSSIAN, S. S., and W. F. STAFFORD. 1979. A reevaluation of the molecular weights and homogeneity of myosin subfragments. *Biophys. J.* **25**:20a (Abstr.).
43. LAUE, T. M., and D. A. YPHANTIS. 1979. Rapid automatic measurement of Rayleigh interferograms from the ultracentrifuge. *Biophys. J.* **25**:164a (Abstr.).
44. STAFFORD, W. F. 1979. Graphical analysis of non-ideal monomer N-mer and isodesmic indefinite self associating systems. *Biophys. J.* **25**:232a (Abstr.).
45. ALBRIGHT, D. A., and J. W. WILLIAMS. 1968. A study of the combined sedimentation and chemical equilibrium of  $\beta$ -lactoglobulin B in acid solution. *Biochemistry*. **7**:67.
46. VISSER, J., R. C. DEONIER, E. T. ADAMS, JR., and J. W. WILLIAMS. 1972. Self-association of  $\beta$ -lactoglobulin in acid solution and its variation with temperature. *Biochemistry*. **11**:2634.
47. GODFREY, J. E., and W. F. HARRINGTON. 1970. Self-association in the myosin system at high ionic strength. II. Evidence for the presence of a monomer = dimer equilibrium. *Biochemistry*. **9**:894.
48. HARRINGTON, W. F., and M. BURKE. 1972. Geometry of the myosin dimer in high salt media. I. Association behavior of rod segments from myosin. *Biochemistry*. **11**:1448.
49. SARQUIS, J. L., and E. T. ADAMS, JR. 1974. The temperature-dependent self-association of  $\beta$ -lactoglobulin C in glycine buffers. *Arch. Biochem. Biophys.* **163**:442.
50. CHUN, S.-Y., W. E. HILL, and P. DOTY. 1978. Characterization of the histone core complex. *Proc. Natl. Acad. Sci. U.S.A.* **75**:1680.